Thin-film transistor behaviour and the associated physical origin of water-annealed In–Ga–Zn oxide semiconductor

2012 J. Phys. D: Appl. Phys. 45 415307

(http://iopscience.iop.org/0022-3727/45/41/415307)

J. Phys. D: Appl. Phys. **45** (2012) 415307 (6pp) doi:10.1088/0022-3727/45/41/415307

Thin-film transistor behaviour and the associated physical origin of water-annealed In–Ga–Zn oxide semiconductor

Byung Du Ahn[1], Jun Hyung Lim[1], Mann-Ho Cho[2], Jin-Seong Park[3] and Kwun-Bum Chung[4]

[1] LCD Business, Samsung Electronics, Gyeonggi-Do 446-711, Korea
[2] Institute of Physics and Applied Physics, Yonsei University, Seoul 120-749, Korea
[3] Material Science and Engineering, Dankook University, Cheonan 330-714, Korea
[4] Department of Physics, Dankook University, Cheonan 330-714, Korea

E-mail: jinseongpark@dankook.ac.kr and kbchung@dankook.ac.kr

Received 22 May 2012, in final form 30 July 2012
Published 28 September 2012
Online at stacks.iop.org/JPhysD/45/415307

Abstract
A transparent In–Ga–Zn oxide semiconductor was thermally annealed in an ambient atmosphere of water vapour and the associated electrical and physical properties of the film were investigated. After annealing in water vapour, the resulting thin-film transistor (TFT) exhibits *n*-type behaviour with a field effect mobility of 11.4 $cm^2\ V^{-1}\ s^{-1}$, and an on/off current ratio of 6.65×10^9. The annealing process in water vapour induces changes in the elemental composition and chemical bonding states of Zn and O. These phenomena affect the changes of band alignment including the band gap and conduction band offset ($\Delta(E_{CB} - E_F)$) of InGaZnO semiconductors, which is the basis for the improved operation and performance of these TFTs.

(Some figures may appear in colour only in the online journal)

1. Introduction

Since Hosono *et al* presented their paper on high performance thin-film transistors (TFTs) with amorphous indium–gallium–zinc-oxide (IGZO) semiconductors [1], much research has shown that oxide TFTs are the best candidates for use in several types of emerging electronics, including active matrix organic light-emitting diodes (AMOLEDs) and transparent/flexible displays [2, 3]. This is because these TFTs have shown high mobility and an excellent gate swing in their amorphous phase. Although there are tremendous efforts in the area of oxide TFT engineering, the material's intrinsic capabilities and limiting factors are yet to be fully understood. Among the factors that many researchers have focused on is trying to understand the relationship between the electrical performance and fabrication process factors, such as the oxygen partial pressure [4], the sputtering power [5], the post-annealing conditions [6, 7], the composition of cations [8] and the contact materials for source/drain materials [9, 10].

In fact, the thermal annealing effect has been essential for understanding the intrinsic nature of amorphous oxide semiconductors in regards to device applications, as this effect is related to the material's physics such as activation energy [11], carrier transport mechanism [12] and density of state (DOS) [13]. Recently, the water processes for oxide TFTs have been adopted to improve the electrical performance and device instability. Groups researching this water processing usually report the changes of device performance and instability depending on water partial pressure [14] and atmosphere [15]. Nomura reported that wet O_2 annealing improves the device performance and reliability of oxide TFT by comparing with dry O_2 annealing [16]. However, in order to understand the fundamental origin of water annealing, we need to systematically investigate the changes of oxide semiconductor using various analysis techniques.

In this work, we investigate the effect of water annealing in oxide TFT using physical and electrical analysis. The annealed InGaZnO film showed changes in cation compositions and

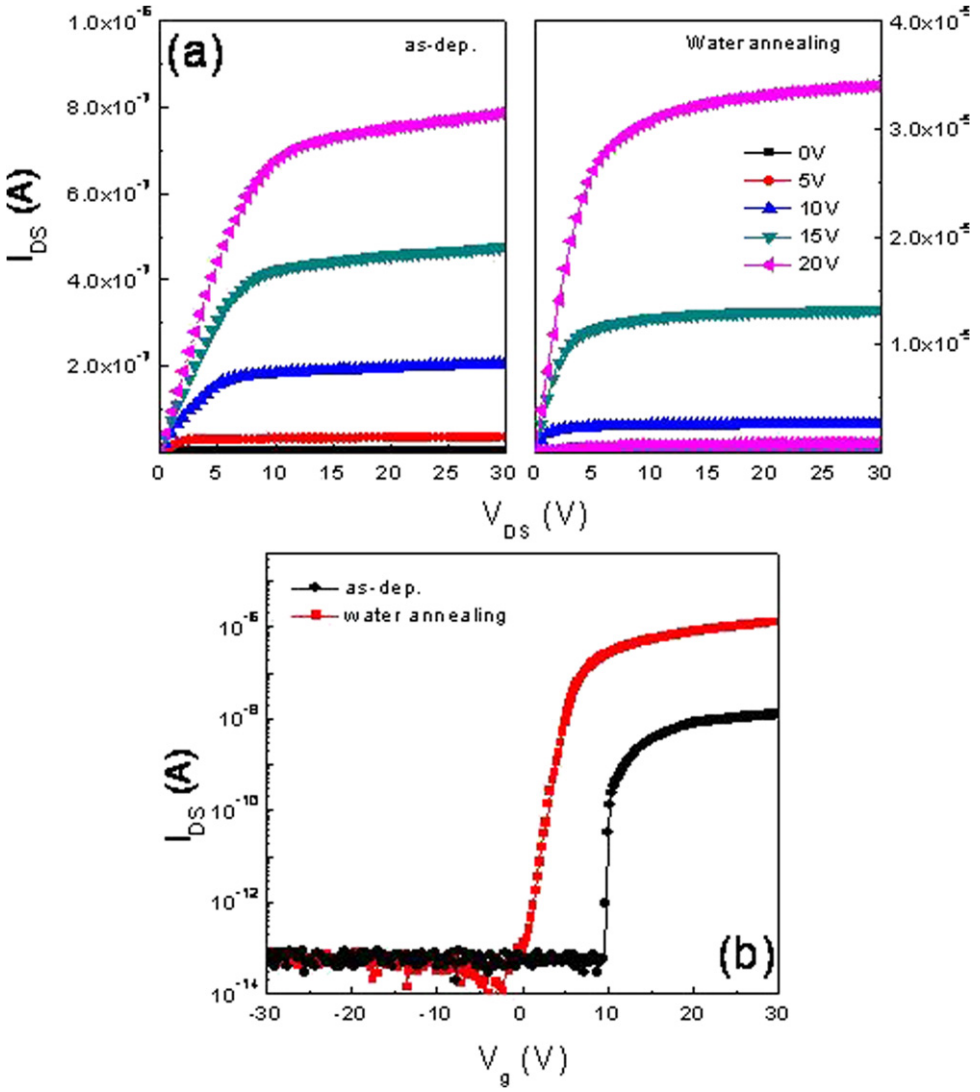

Figure 1. Representative (*a*) output and (*b*) transfer characteristics of the as-deposited and water-annealed InGaZnO-based TFTs with $W/L = 40/20\,\mu$m.

additional OH speices, which could be related to carrier concentration and Hall mobility. In addition, the physical origin of water annealing was investigated by looking at the electronic band alignments of InGaZnO film.

2. Experiment

The Ti/Cu was deposited and patterned on a glass substrate by dc sputtering and wet etching for use as the gate electrode. Then, 400 nm thick SiN_x and 50 nm thick SiO_x were deposited as gate insulators by plasma-enhanced chemical vapour deposition (PECVD) at 370 °C. For the active layer, 40 nm thick amorphous-InGaZnO (In : Ga : Zn = 1 : 1 : 1 at%) was deposited by dc sputtering at 100 °C with oxygen partial pressure of 0.02 Torr using Ar and O_2 gas. After that, the samples were annealing at 300 °C for 1 h in a water vapour ambient atmosphere, which is made using a combination of H_2 and O_2 gas. The ratio ($H_2 : O_2$) was 3 : 2 and the process pressure was kept at 1 atm. Then, the etch stopper SiO_x layer with a 50 nm thickness was added and patterned by dry etching. The source/drain (S/D) electrodes, Ti/Cu, were deposited and patterned using dc sputtering and dry etching. Finally, in order to avoid contamination of the prepared InGaZnO-based TFT, SiN_x was deposited as a passivation layer by PECVD.

The separated InGaZnO films were prepared on identical substrates and subjected to the same heat treatments as the TFT devices. The changes in composition and chemical bonding states were investigated by Rutherford backscattering spectroscopy (RBS), x-ray photoelectron spectroscopy (XPS) and time-of-flight secondary ion mass spectroscopy (TOF-SIMS). TOF-SIMS was recorded by the sputtering of 2 keV–100 nA Cs^+ ion beam and the data acquisition of 25 keV–1 pA Bi_3^+ ion beam with the incident angle of 40°. The band alignments including the band gap and band offset were examined by spectroscopic ellipsometry (SE) and XPS.

3. Results and discussion

Figure 1 shows the electrical characteristics of the as-deposited and water-annealed InGaZnO-based TFTs: (*a*) the output

Table 1. Device parameters including μ_{FE}, V_{th}, SS and the $I_{on/off}$ ratio for the as-deposited and water-annealed InGaZnO-based TFTs.

	μ_{FE} ($cm^2\ V^{-1}\ s^{-1}$)	V_{th} (@1 nA)	SS (V/dec)	$I_{on/off}$ ratio
As-deposited	1.12	10	0.21	4.48×10^7
Water annealing	11.4	3	0.76	6.65×10^9

characteristics and (*b*) the representative transfer characteristics. The as-deposited InGaZnO-based TFTs showed the lower on-current and higher threshold voltage. However, the water-annealed InGaZnO-based TFTs produced moderated transistor behaviour and a saturated I_{DS} was observed with a clear pinch-off, which implies that the electron transport in the water-annealed InGaZnO active channel is controlled by the gate and drain voltages. The μ_{FE} was determined by the maximum trans-conductance at a drain voltage (V_{DS}) of 10 V, and the V_{th} was determined by the gate voltage (V_{GS}) required to produce a drain current of $L/W \times 1$ nA at $V_{DS} = 10$ V. The subthreshold gate swing ($SS = dV_{GS}/d \log I_{DS}$) was extracted from the linear portion of the plot of $\log I_{DS}$ versus V_G. The device performances of the as-deposited and water-annealed InGaZnO TFT are summarized in table 1 for μ_{FE}, V_{th}, SS and I_{on}/I_{off} ratio. After water annealing, InGaZnO TFT has the higher field-effect mobility and I_{on}/I_{off} ratio. In order to study the electrical properties such as carrier concentration and Hall mobility of InGaZnO films, Hall measurements were carried out using van der Pauw configuration (dc measurement mode, magnetic field = 0.499 T) at room temperature. The Hall mobility and carrier concentration are 13 $cm^2\ V^{-1}\ s^{-1}$ and $3 \times 10^{16}\ cm^{-3}$ for water-annealed InGaZnO films, and the values below the detection limit ($\sim 1 \times 10^{14}\ cm^{-3}$) for the as-deposited InGaZnO film. Even if these values of InGaZnO thin films are strongly connected to the device performance, it is difficult to solve the fundamental origin of the semiconducting properties of water-annealed InGaZnO film. The following results and discussion are provided to help understand the operation and performance of water-annealed InGaZnO TFT. This is achieved by comparing between the as-deposited InGaZnO film and the water-annealed InGaZnO film in conjunction with physical property analysis.

In order to obtain a change of stoichiometry after water annealing, RBS measurements were performed using 2 MeV He^{2+} ions with a scattering angle of 170°. Figure 2 shows the backscattering results of the He^{2+} ions for the as-deposited and water-annealed InGaZnO films with a thickness of 50 nm. Even though the peaks of Zn and Ga are overlapped, the detailed amount of In, Ga, Zn, and O could carefully be calculated with the resolution of $\sim 1 \times 10^{16}$ atoms cm^{-2} using RUMP code. The relative atomic concentrations are summarized in table 2. One finding of interest is the minute increase in O composition and the slight decrease in Zn composition, after water annealing of the as-deposited InGaZnO film.

The detailed variations of the elemental composition and binding were investigated by TOF-SIMS, as shown in figure 3 for (*a*) H^+, (*b*) OH^-, (*c*) ZnO^+, (*d*) O_2, (*e*) GaO^+ and (*f*) InO^+. The water annealing process causes drastic increases in

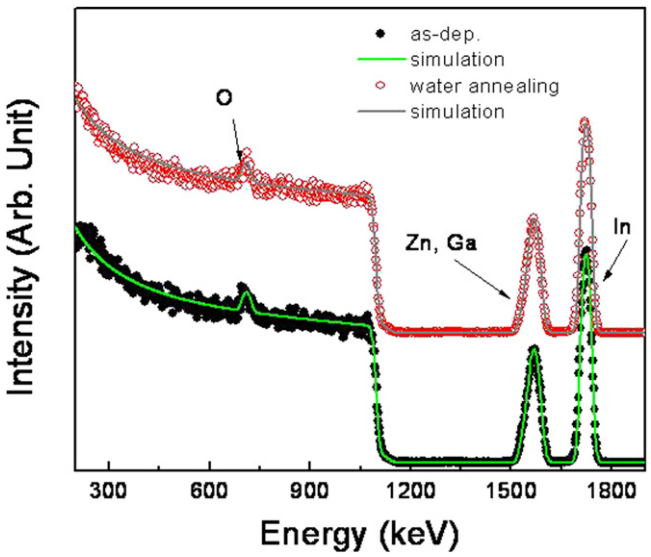

Figure 2. RBS data of the as-deposited and water-annealed InGaZnO films. Dots and lines are raw data and simulation results using the RUMP code, respectively.

H^+ and OH^- contents, and slight decreases in ZnO^+ content, comparing with the variations in the other binding contents (O_2, GaO^+, InO^+). The higher content of H^+ and OH^- in the top film region is caused by the surface contamination of the H_2O in air during *ex situ* measurements. These characteristics related to O and Zn are consistent with the stoichiometric results shown in figure 2. More specifically, the increase in O is related to hydrogen and the decrease in Zn is related to oxygen, this means a relative decrease in the stoichiometric binding of Zn and O. Even if wet O_2 annealing suppresses the desorption of Zn–O components rather than dry O_2 annealing [16], the annealing process could induce the stabilization of unstable chemical bond through the desorption, such as the decrease in the ZnO content. The relative increase of hydrogen in the water-annealed InGaZnO film can be considered as a result of the incorporation of H or deoxidization via water annealing.

In addition to the quantitative analysis by RBS and TOF-SIMS measurements, changes in the chemical bonding characteristics after water annealing are crucial evidence in understanding the physical and electrical properties of water-annealed InGaZnO film. In particular, the chemical bonding states of oxygen, shown in figure 4, are the main bonding state of InGaZnO film. In order to eliminate the surface contamination by adsorbed OH, C, H_2O, etc and minimize the preferred sputtering of light elements, XPS measurements were carried out after sputtering using Ne ions at 500 eV. The water-annealed InGaZnO film has a higher bonding state, at around 532.5 eV, compared with the as-deposited InGaZnO film. In order to examine the detailed oxygen states, the O 1s spectra were carefully deconvoluted into three peaks (O1, O2, O3) using Gaussian fitting with the subtraction of a Shirley type background and by considering the previous report [17]. The O1 peak in the low binding energy of the O 1s spectrum is attributed to O^{2-} ions on the metal oxides, indicating In–Ga–Zn–O bonds [18]. The higher binding energy (O3) around 533.5 eV is usually attributed to chemisorbed or dissociated oxygen or OH species on the

Table 2. Atomic concentration and relative percentage of the as-deposited and water-annealed InGaZnO films, measured by RBS.

	O	Zn	Ga	In
As-dep.	1.85×10^{17} (54.4%)	0.42×10^{17}(12.4%)	0.58×10^{17}(17.1%)	0.55×10^{17}(16.1%)
Water annealed	2.14×10^{17}(58.0%)	0.37×10^{17}(10.0%)	0.61×10^{17}(16.5%)	0.57×10^{17}(15.5%)

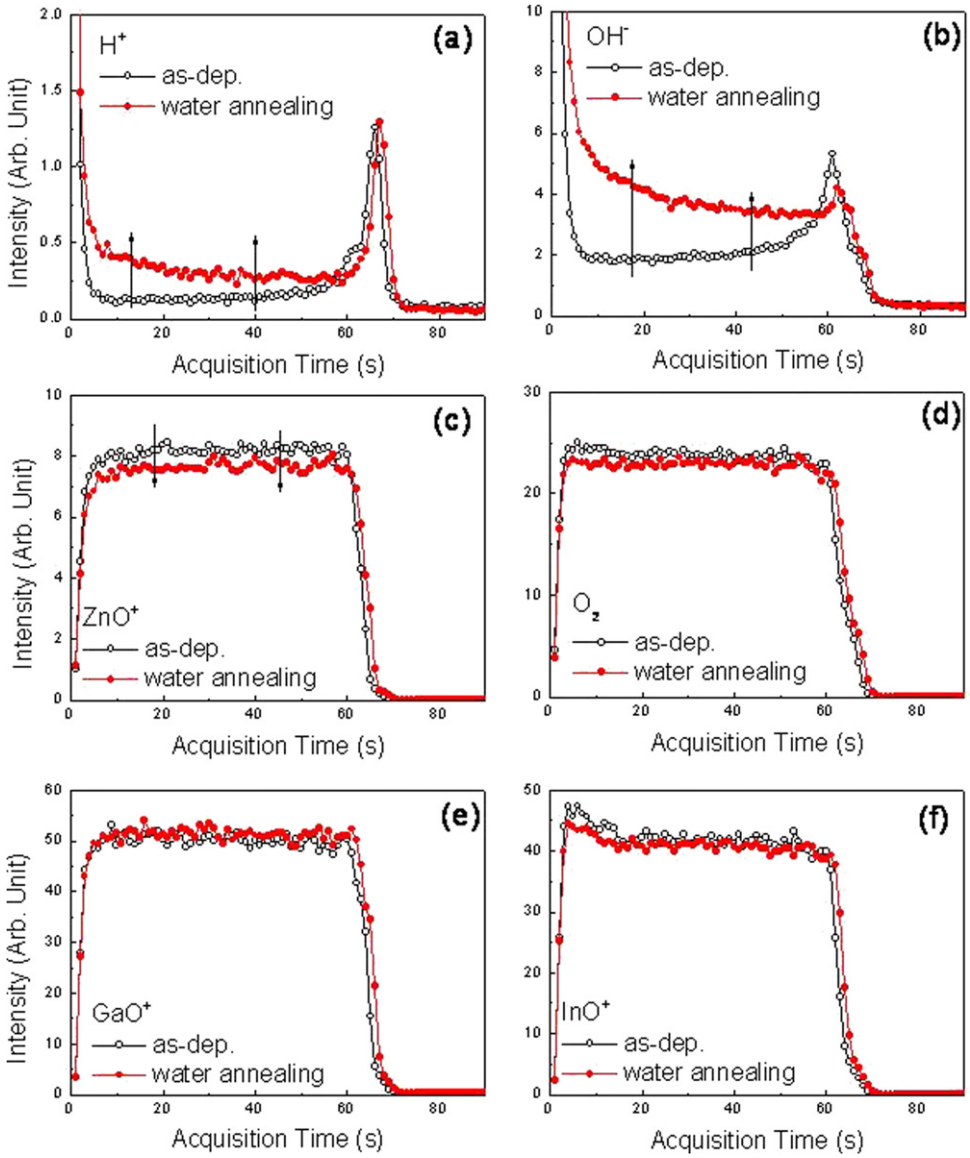

Figure 3. TOF-SIMS spectra in the depth direction of the as-deposited and water-annealed InGaZnO films for (*a*) H^+, (*b*) OH^-, (*c*) ZnO^+, (*d*) O_2, (*e*) GaO^+ and (*f*) InO^+.

surface of the InGaZnO films, such as -CO_3, adsorbed H_2O or adsorbed O_2. The component at the medium binding energy (O2) of the O 1s spectrum is associated with OH bonding species and with O^{2-} ions that are in the oxygen-deficient In–Ga–Zn–O bonding matrix [19, 20]. The relative ratio of O2 peak between as-deposited and water-annealed InGaZnO films is increased by ∼50%, which corresponds to the increase in ∼5.3% in the entire film composition including In, Ga, Zn and O. As a result, changes in the intensity of the O2 peak may be connected with the OH bonding state and with the variations in the concentration of the oxygen vacancies (V_O). Based on the above analysis, we can say that water annealing induces the increase in OH bonding states or the oxygen vacancies. Even though the quantification of individual contribution of OH bonding states and oxygen vacancy to the electrical enhancement is indefinite, the formation of OH bonding states and oxygen vacancies is able to generate the charge carrier, due to the increase of free electron [21, 22]. In addition, the increase of oxygen vacancies corresponds to previous RBS and TOF-SIMS results from the of viewpoint of the lesser ZnO bonding state, this can lead to the electrically metallic properties [18].

Figures 5(*a*), (*b*) and (*c*) show the bandgap and valence band spectra measured by SE and XPS, and the schematic

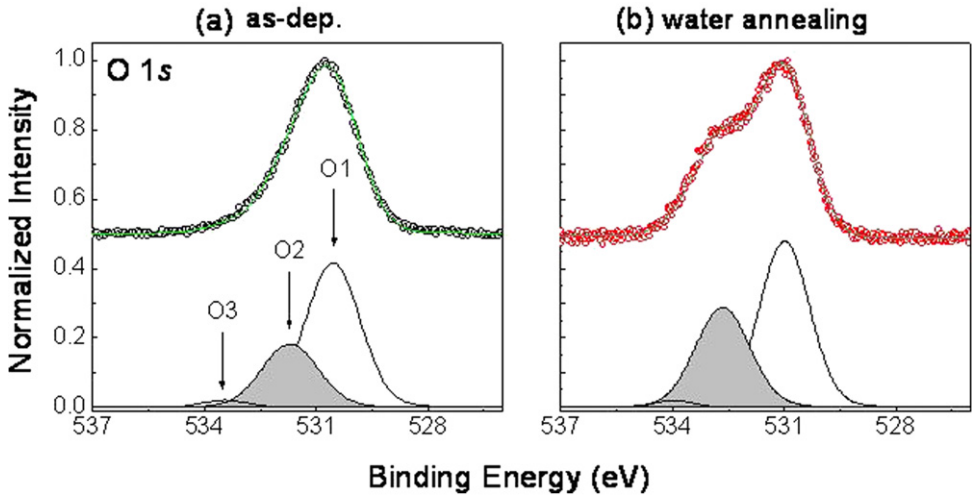

Figure 4. The O 1s XPS core-level spectra of the as-deposited and water-annealed InGaZnO films. The deconvoluted peaks near ∼530 eV and ∼532 eV are denoted as a metal oxide peak and a OH peak or oxygen vacancy, respectively.

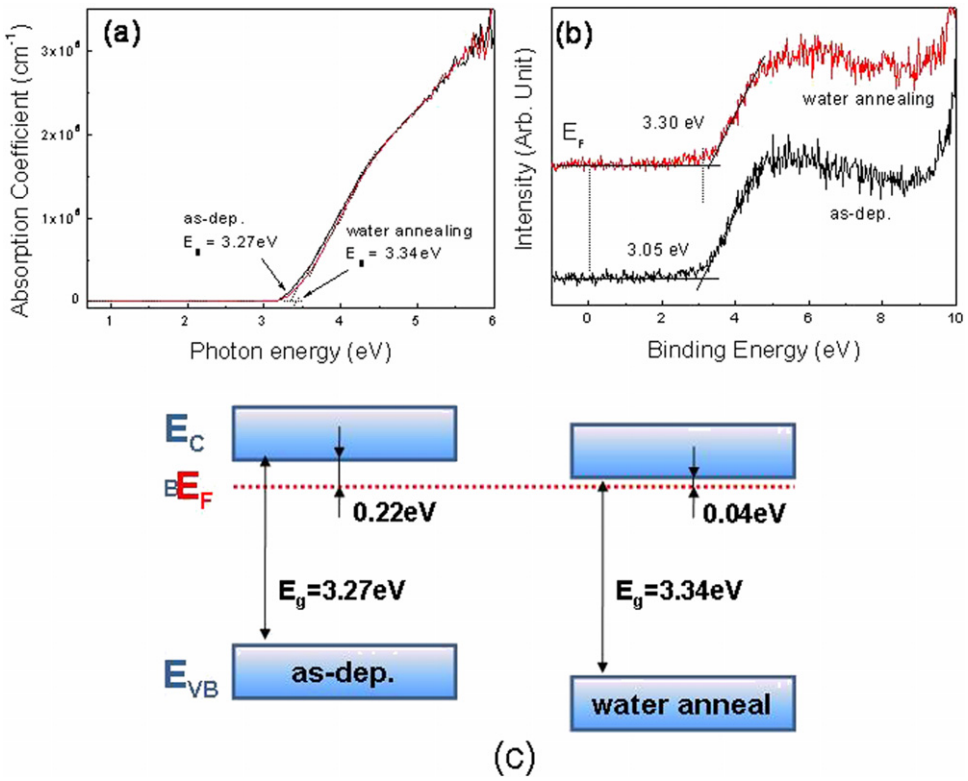

Figure 5. (*a*) Absorption coefficient spectra of the as-deposited and water-annealed InGaZnO films. (*b*) Valence band spectra of the as-deposited and water-annealed InGaZnO films. (*c*) Energy level diagram of the as-deposited and water-annealed InGaZnO films.

Table 3. Energy alignment of the as-deposited and water-annealed InGaZnO films for band gap (E_g), valence band offset ($\Delta(E_{VB} - E_F)$), and conduction band offset ($\Delta(E_{CB} - E_F)$).

	E_g	$\Delta(E_{VB} - E_F)$	$\Delta(E_{CB} - E_F)$
As-dep.	3.27 eV	3.05 eV	0.22 eV
Water annealed	3.34 eV	3.30 eV	0.04 eV

energy diagram for the as-deposited and water-annealed InGaZnO films. The bandgap (E_g), conduction band offset ($\Delta(E_{CB} - E_F)$) and valence band offset ($\Delta(E_{VB} - E_F)$) are summarized in table 3. After water annealing, the bandgap is slightly increased from 3.27 to 3.34 eV and the valence band offset is also increased. This results in the drastic decrease in the conduction band offset from 0.22 to 0.04 eV, which is strongly correlated with the carrier concentration [23]. Based on the above results, the most plausible origin of improved device operation and performance in water-annealed InGaZnO TFTs may be attributed to the increase in carrier concentration in the water-annealed InGaZnO channel layer as a result of the reduction of the conduction band offset by the changes in the elemental composition and bonding states of oxygen.

4. Conclusions

A transparent In–Ga–Zn oxide semiconductor was thermally annealed in an ambient atmosphere of water vapour and the associated electrical and physical properties of the film were investigated. The thin-film transistor produced using water-annealed In–Ga–Zn oxide exhibits n-type behaviour with a field-effect mobility of 11.4 $cm^2\ V^{-1}\ s^{-1}$, and an on/off current ratio of 6.65×10^9, respectively. The elemental composition related to Zn and O is changed after the water annealing process. The water-annealed In–Ga–Zn oxide shows a smaller content of ZnO and a larger content of OH in the entire oxide film. In addition, the chemical bonding states of oxygen indicate the increase of OH states or oxygen vacancies. These variations in the physical characteristics due to water annealing affect the band alignments including the band gap and conduction band offset ($\Delta(E_{CB} - E_F)$) of In–Ga–Zn oxide semiconductors, which is the basis of the improved operation and performance of these thin-film transistors.

Acknowledgments

This research was partially supported by the Basic Science Research Program through the National Research Foundation of Korea (NRF) funded by the Ministry of Education, Science and Technology (2012-0002430 and 2012-0002041). In addition, the LCD division of Samsung Electronics Inc. partially supported this work financially.

References

[1] Nomura K, Ohta H, Takagi A, Kamiya T, Hirano M and Hosono H 2004 *Nature* **432** 488
[2] Park J, Maeng W J, Kim H S and Park J S 2012 *Thin Solid Films* **520** 1679
[3] Park J S, Kim T W, Stryakhilev D, Lee J S, An S G, Pyo Y S, Lee D B, Mo Y G, Jin D U and Chung H K 2009 *Appl. Phys. Lett.* **95** 013503
[4] Suresh A, Gollakota P, Wellenius P, Dhawan A and Muth J F 2008 *Thin Solid Films* **516** 1326
[5] Chiang H Q, McFarlane B R, Hong D, Presley R E and Wager J F 2008 *J. Non-Cryst. Solids* **354** 2926
[6] Hosono H, Nomura K, Ogo Y, Uruga T and Kamiya T 2008 *J. Non-Cryst. Solids* **354** 796
[7] Shin H S, Ahn B D, Kim K H, Park J S and Kim H J 2009 *Thin Solid Films* **517** 6349
[8] Iwasaki T, Itagaki N, Den T, Kumomi H, Kamiya T and Hosono H 2007 *Appl. Phys. Lett.* **90** 242114
[9] Barquinha P, Vila A, Goncalves G, Pereira L, Martins R, Morante J and Fortunato E 2008 *IEEE Trans. Electron Devices* **55** 954
[10] Shimura Y, Nomura K, Yanagi H, Kamiya T, Hirano M and Hosono H 2007 *Thin Solid Films* **516** 5899
[11] Takechi K, Nakata M, Eguchi T, Yamaguchi H and Kaneko S 2009 *Japan. J. Appl. Phys.* **48** 011301
[12] Kamiya T, Nomura K and Hosono H 2009 *J. Disp. Technol.* **5** 468
[13] Jeong J, Jeong J K, Park J S, Mo Y G and Hong Y 2010 *Japan. J. Appl. Phys.* **49** 03CB02
[14] Aoi T, Oka N, Sato Y, Hayashi R, Kumomi H and Shigesato Y 2010 *Thin Solid Film* **518** 3004
[15] Park J S, Jeong J K, Chung H J, Mo Y G and Kim H D 2008 *Appl. Phys. Lett.* **92** 072104
[16] Nomura K, Kamiya T, Ohta H, Hirano M and Hosono H 2008 *Appl. Phys. Lett.* **93** 192107
[17] Hsieh P-T, Chen Y-C, Kao K-S and Wang C-M 2008 *Appl. Phys.* A **90** 317
[18] Lee M J, Kang S-J, Baik J Y, Kim K-J, Kim H-D, Shin H-J, Chung J, Lee E, Lee J and Lee J 2010 *Electrochem. Solid-State Lett.* **13** H454
[19] Moon J C, Aksoy F, Ju H, Liu Z and Mun B S 2011 *Curr. Appl. Phys.* **11** 513
[20] Szörényi T, Laude L D, Bertóti I, Kántor Z and Geretovszky Zs 1995 *J. Appl. Phys.* **78** 6211
[21] Kamiya T, Nomura K and Hosono H 2009 *J. Disp. Technol.* **5** 273
[22] Hyun-woo Park, Jin-Seong Park, Ju Ho Lee and Kwun-Bum Chung 2012 *Electrochem. Solid-State Lett.* **15** H133
[23] Park J, Ok K C, Ahn B D, Lee J H, Park J-W, Chang K-B and Park J S 2011 *Appl. Phys. Lett.* **99** 142104